MECHANICAL PROPERTIES OF POLYPROPYLENE FIBER REINFORCED HIGH-STRENGTH CONCRETE EXPOSED TO ELEVATED TEMPERATURES: AN EXPERIMENTAL AND ARTIFICIAL NEURAL NETWORK APPROACH

Fahim Shahriar*[1], Bokul Roy[2] and Shuvo Dip Datta[3*]

[1]*Graduate Student, Khulna University of Engineering & Technology, Bangladesh, e-mail: tfahim645@gmail.com*
[2]*Graduate Student, Khulna University of Engineering & Technology, Bangladesh, e-mail: bokulroy0471@gmail.com*
[3*]*Lecturer, Khulna University of Engineering & Technology, Bangladesh, e-mail: sd.datta@becm.kuet.ac.bd*

***Corresponding Author**

ABSTRACT

This paper evaluates the mechanical characteristics of polypropylene-based High-Strength Concrete (HSC) when exposed to various elevated temperatures. This complete approach was structured into two phases. The primary objectives of phase one encompassed material characterization for the experiment and involved an examination of both the fresh and hardened characteristics of concrete. In the second phase, a Multi-layer Perceptron, also known as the Artificial Neural Network (ANN) model, was developed as a strength prediction model for HSC. The model's precision was ensured through the assessment of the mean absolute error (MAE), mean square error (MSE), and root mean square error (RMSE). A total of four different concrete compositions were prepared, each with varying polypropylene fiber (PPF) contents of 0.5, 1.0, and 1.5 kg/m^3 of concrete. These compositions were then exposed to 150°C, 350°C, 550°C, and 750 °C temperatures, respectively. The hardened properties of HSC were examined through compressive and tensile strength tests over 28 days at all elevated temperatures. The findings of these experiments indicated a decline in fresh properties, while an enhancement was observed in the mechanical behavior of HSC with the addition of PPF. Additionally, elevated temperatures led to a reduction in the mechanical performance of all HSC mixes, but the incorporation of fibers noticeably mitigated the strength loss. 1.0 kg/m^3 of PPF was found to be the optimum inclusion. Finally, in phase two, a data augmentation technique was applied to extend the experimental dataset to introduce variability while training the ANN model. In addition to that, two separate regularization methods were also employed to find the best possible approach to reduce overfitting, aiming to build an improved prediction model. The achievement of a high linear coefficient correlation (R^2) value of 0.957 with the unseen testing dataset underscores the superior performance of the selected ANN model.

Keywords: *High-strength concrete, Polypropylene fiber, Elevated temperature, Artificial neural network, Data augmentation.*

1. INTRODUCTION

The adoption of HSC in constructing structural elements is on the rise across the globe because of the number of benefits offered by such concrete. HSC has higher physico-mechanical qualities such as compressive strength, stiffness, and long-term durability, as well as cost benefits from geometrical section reductions (Hamrat et al., 2010). However, HSC is known to have adverse effects on its mechanical properties and leads to explosive spalling when it is exposed to high temperatures (Elsanadedy et al., 2017). The spalling occurs in HSC due to the reduced water-cement ratio and permeability of the concrete (Noumowe et al., 2009). The HSC experienced significant strength loss at nearly 150ºC due to the high pore pressure impact caused by the low permeability of HSC (Bangi & Horiguchi, 2011). Some researchers (Long & Nicholas, 2001) found that the dense microstructure of HSC caused by the low W/C ratio provides the HSC a poor permeability, preventing the release of water vapor within the pores as the temperature rises, making the concrete more prone to spalling. According to Caetano et al. (2019) in the temperature range of 700 to 900 degrees Celsius, concrete undergoes substantial mass loss and critical transformations, including decarbonization of limestone aggregates, resulting in compromised microstructural strength and reduced mechanical resistance.

It is widely known that the participation of fibers is the most effective means of preventing HSC from spalling (Choumanidis et al., 2016). In comparison to other fibers, the inclusion of polypropylene in HSC shows better performance in terms of mechanical properties at elevated temperatures and its shrinkage control (Bilodeau et al., 2004; Kalifa et al., 2001; Roy et al., 2021; Serrano et al., 2016). PPF incorporated in concrete creates pores and small channels when exposed to elevated temperatures with the fiber melting. The additional porosity and small channels lower internal vapor pressures in the concrete and reduce the chance of spalling (Noumowe, 2005). According to several authors (Bilodeau et al., 2004; Varona et al., 2018), PPF melts at 160–170 ºC and vaporizes at 350 ºC, introducing new pores and microcracks in the cementitious matrix that may improve concrete's permeability. These phenomena reduce the damage and resistance of the concrete exposed to high temperatures of the fire (Ozawa & Morimoto, 2014). Behnood and Ghandehari (2009) observed that High-strength concrete (HSC) containing PPF showed significant compressive and splitting tensile strength at normal temperature (25°C). Nevertheless, HSC having PPF demonstrated a greater percentage of retained compressive strength compared to other mixtures when subjected to elevated temperatures. Huismann et al. (2012) noticed that the addition of PPF accelerated moisture transport in HSC. For that, the transient strain under 750°C resulted in drying shrinkage occurring in the reverse direction of the free heat stress.

Compressive strength is the most crucial property to investigate the strength of concrete and is widely used in the construction sectors (Tanyildizi & Coskun, 2008). However, determining this characteristic often involves a prolonged trial-and-error process. An effective approach is the utilization of cutting-edge technology, such as Machine Learning (ML) algorithms. These algorithms take various concrete parameters as input and make predictions on strength with a certain level of precision. Many authors (Abuodeh et al., 2020; Ahmadi et al., 2017) applied ANN to analyze compressive strength forecasting abilities and recommended it for future experiments. In a study, Almohammed and Thakur (2023) investigated the strength predictive capabilities of concrete mixed with Basalt Fiber and PPF using different ML models. Similarly, Altun and Dirikgil (2013) and Uddin et al. (2023) also evaluated different algorithms to explore alternative ways to determine mechanical characteristics under elevated temperatures and dynamic yield stress of PPF-reinforced concrete. Significant outputs of different evaluation metrics confirmed their analytical abilities in real-world scenarios.

In this study, the authors experimented with different temperatures' effects on the fresh and hardened properties of PPF-reinforced HSC and established a robust ANN model, counterfeiting the possibilities of overfitting through the augmented dataset along with regularization techniques. While several studies have explored the heat impact on concrete containing PPF, no analysis has been noticed specifically investigating the application of ANN models trained using an extended dataset for

PPF-reinforced HSC. This novel approach not only added uniqueness but also enabled opportunities for a more comprehensive exploration of concrete technology through advanced ML techniques.

2. METHODOLOGY

2.1 Materials

In this study, Ordinary Portland Cement (OPC) type I (CEM-I 52.5 N) was manufactured by a regional brand in compliance with ASTM C150 (2020). River sand, having a fineness modulus of 2.77 as per ASTM C136 (2019), was employed as the fine aggregate in the concrete blends. On the other hand, crushed stone chips with a maximum nominal size of 19 mm were used as the coarse aggregate. The specific gravity and water moisture content of the coarse and fine aggregates were 2.82, 1.78% and 2.45, 2.31%, respectively. The results of the investigation of various aggregate grades using the ASTM (C29, 2017; C127, 2015; C128, 2015) standards are highlighted in Table 1. A polycarboxylate-based ether was used as a superplasticizer (SP) to tune the workability of the concrete mixes. PPF with lengths and diameters of 12 mm and 24 µm, respectively, were utilized in the study, which followed the standard of ASTM C1116 (2015). Table 2 shows the fiber properties.

Table 1: Aggregate properties

Properties	Specific gravity	Absorption (%)	Moisture content (%)	Unit weight (kg/m^3)		Void ratio (%)	
				Compacted	Loose	Compacted	Loose
Coarse Aggregate	2.82	1.17	1.78	1671	1494	38.2	44.8
Fine Aggregate	2.45	1.63	2.31	1563	1393	34.5	41.9

Table 2: PPF properties

Diameter	Tensile strength	Specific gravity	Absorption	Modulus of elasticity	Melting point	Ignition point	Alkali, acid, and salt resistance
24 µm	550 MPa	0.91	None	3447 MPa	160°C	590°C	High

2.2 Mix Proportion

In accordance with ASTM C192 (2019), four different concrete mixes were established with varying dosages of PPF amounted to 0, 0.5, 1.0, and 1.5 kg/m^3 of concrete. The total mix designs are shown in Table 3. Cylindrical testing samples with a diameter of 100 mm and height of 200 mm were made and preserved in the laboratory at 25°C (room temperature) for 24 hours. After initial hardening, the samples went through a 28-day curing process in water tanks before being subjected to elevated temperatures, including 150°C, 350°C, 550°C and 750°C at a heating rate of 18°C/min using an electric furnace. The specimens were kept at designated temperatures for 30 minutes and cooled to room temperature by the end. Throughout the process, a digital controller with a microprocessor-based PID system was utilized to maintain higher temperatures in the furnace.

Table 3: Mix design of concrete specimens

Specimens code	Cement (kg/m^3)	Fine Aggregate (kg/m^3)	Coarse Aggregate (kg/m^3)	Fiber content (kg/m^3)	W/C	Water (kg/m^3)	SP (%)
HSC	532	804	844	0	0.3	159	1
FRHSC-0.5	532	804	844	0.5	0.3	159	1
FRHSC-1.0	532	804	844	1	0.3	159	1
FRHSC-1.5	532	804	844	1.5	0.3	159	1

2.3 Test Methods

To analyse the fresh properties of the concrete mixes, the slump and compacting factor tests were carried out following ASTM C143 (2015), and BS 1881-103 (1993) standards, respectively. After treating the specimens with different temperatures, mechanical characteristics were recorded in compliance with ASTM C39 (2020) for compressive and ASTM C496 (2017) for splitting tensile strength tests at 28 days.

2.4 ANN Model

Artificial Neural Networks (ANNs) are constructed on computational frameworks, mirroring the biological mechanisms of the human brain's neural system, which processes information through interconnected neurons. Likewise, ANNs consist of layers of artificial neurons (also known as nodes) that work together to solve complex problems and make predictions. The capacity of ANNs to rapidly acquire proficiency in addressing intricate problems has been demonstrated through recent breakthroughs in artificial intelligence (LeCun et al., 2015). Typically, a neural network consists of three layers, including the input layer, hidden layers, and output layer, where neurons within the same layer are not directly connected. The input layer represents input parameters, and the number of input neurons matches the problem's output neurons. Hidden layers are mainly used in facilitating intermediate processing of the data between the input and output layers. In this experiment, different PPF content and varying temperatures were used as input variables, with compressive strength as the output feature. Several neural network models were constructed with the Rectified Linear Unit (ReLU) (Agarap, 2018) activation function in the hidden layers, whereas a linear transfer function was employed in the output layer. Before conducting cross-validation, the Adaptive Moment Estimation (Adam) (Singarimbun et al., 2019) optimizer was utilized in conjunction with backpropagation to train the neural network with all the architectures. Subsequently, based on the validation result, an optimal ANN structure comprising two hidden layers with four nodes in the first and three nodes in the subsequent hidden layers, respectively, was determined with proper adjustment in hyperparameters. The architecture is illustrated in Figure 1.

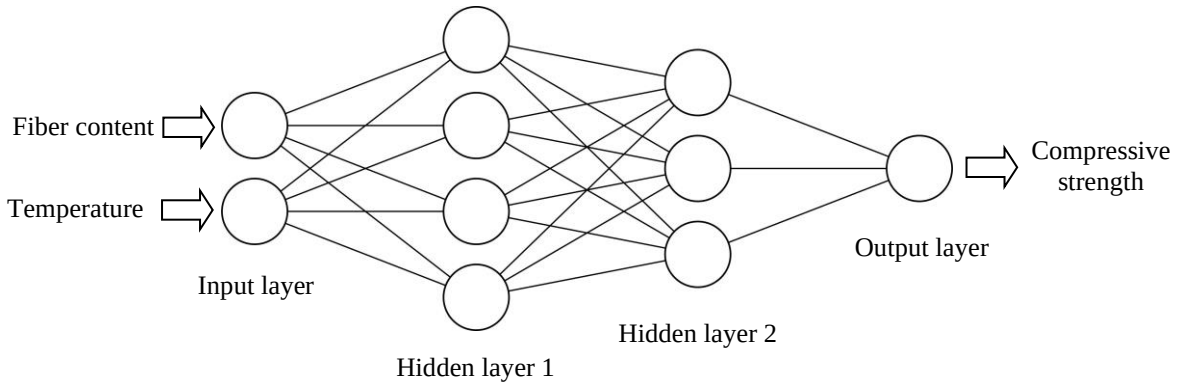

Figure 1: Selected model’s layout (LeNail, 2019).

2.4.1 Data Augmentation

When complex ML models like ANNs are fed with small datasets for training, the challenge of overfitting is magnified as the models may struggle to learn meaningful patterns. To address such issues, the data augmentation approach can be an effective solution to enhance the models' generalization abilities (Ying, 2019). Similarly, it is also crucial to ensure appropriate augmentation techniques for realistic sample generation (Meyer et al., 2021). A comprehensive study of Gaussian Copula augmentation by El Khessaimi et al. (2023) noticed a boost in performance with 500 simulated data points. For our experiment, Gaussian Noise (GN) augmentation was incorporated to introduce 150 synthetic samples. It is a repeated process that employs a normal distribution with 0 as the mean and a specific standard deviation (std), which is then added independently to each data point. The magnitude of the noise is controlled by adjusting the std. In this study, different std values

were iteratively tried based on the correlation between the original data points, and optimum values were determined. Equation 1 demonstrates the mathematical formula of GN.

$$X_a = X_o\, N(\mu, \sigma) \quad (1)$$

In the context of data augmentation, X_a represents the augmented data point, while X_o denotes the original data point. The notation N(μ, σ) is used to describe a randomly extracted sample from a Gaussian distribution, where μ denotes the mean and σ denotes the std.

3. RESULTS AND DISCUSSION

3.1 Fresh Properties

The workability of the mixes was determined through the slump and compacting factor test. The findings are visually illustrated in Figure 2. There was a significant decline in slump value was noted with the inclusion of PPF. The control sample HSC yielded 90 mm in a slump, followed by FRHSC-0.5, FRHSC-1.0, and FRHSC-1.5, with a reduction of approximately 17%, 22%, and 40%, respectively. Other studies also highlighted similar traits of fibers in terms of reducing the slump (Afroughsabet & Ozbakkaloglu, 2015; Nath et al., 2021; Shahriar et al., 2022). PPF was found to be responsible for making the mixtures adhere and cohesive, leading to a reduction in the slump value. Similarly, the compacting factor value followed the same downward trend with the increment of fiber volume. A compacting factor of 0.85 was gained by the control HSC, while FRHSC-0.5, FRHSC-1.0, and FRHSC-1.5 encountered a slight reduction of 2%, 4% and 7%, respectively, in the same order.

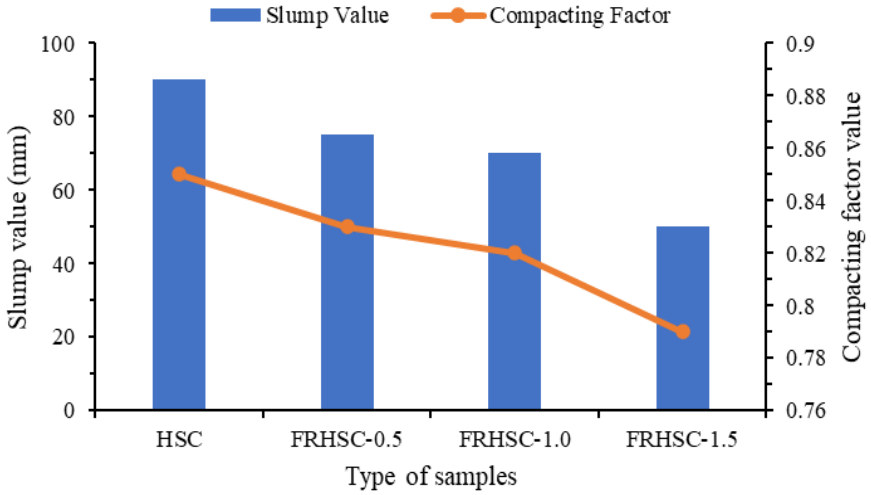

Figure 2: Fresh test results of the mixes

3.2 Mechanical Properties

3.2.1 Compressive Strength Behavior

The outcomes of the compressive strength test of HSC mixtures for various content of PPF (0.5, 1.0 and 1.5 kg/m^3) at different temperatures (150°C, 350°C, 550°C and 750°C) for 28 days are presented in Figure 3. It is noticeable that the participation of PPF in the concrete mixtures improves their compressive strength. However, the temperature significantly impacted compressive strength reduction by about 22-55% for mixture HSC, 14-50% for FRHSC-0.5, 13-45% for HSC-1,0, and 14-46% for FRHSC-1.5 at temperatures of 150°C, 350°C, 550°C, and 750°C respectively, in comparison to the room temperature. The result also shows that normal HSC mixes demonstrated more vulnerability at elevated temperatures relative to HSC specimens containing PPF. Similar findings were recorded regarding the decrease in strength of HSC at higher heat exposure in earlier analysis (Kalifa et al., 2001). According to Behnood and Ghandehari (2009), specimens with 0, 1, 2, and 3 kg/m^3 PPF content respectively, demonstrated a noticeable reduction of about 15–73%, 13–70%, 11–

69%, and 12–71% in relative strength of concrete at 100–600°C in comparison to room temperature. In our investigation, after heating the testing samples at 150°C, mixture HSC showed the maximum loss in compressive strength, whereas the FRHSC-1.0 showed the lowest relative loss in contrast to the standard temperature (25°C). In a similar manner, both the HSC and FRHSC-1.0 mixes showed the most significant and least significant declines in strength at temperatures of 350°C, 550°C, and 750°C among all the mixtures. After being exposed to 750°C, all HSC specimens showed a significant drop in compressive strength. The noted decrease under higher temperatures is likely due to a combination of factors, including the disintegration of Ca(OH)2 and the deterioration of the cohesion between aggregates and cement paste. This weakening results from both the expansion of aggregates and the corresponding contraction of the paste, coupled with the drop in moisture. In contrast, the presence of PPF significantly mitigated the adverse effects of high temperatures over the strength loss in HSC mixes. After crossing 160°C, PPF melted, forming channels for the release of pore vapor. This gradual release of vapor helped lower the temperature and, in turn, minimized the formation of microcracks within the concrete. Consequently, the performance was enhanced under high temperatures.

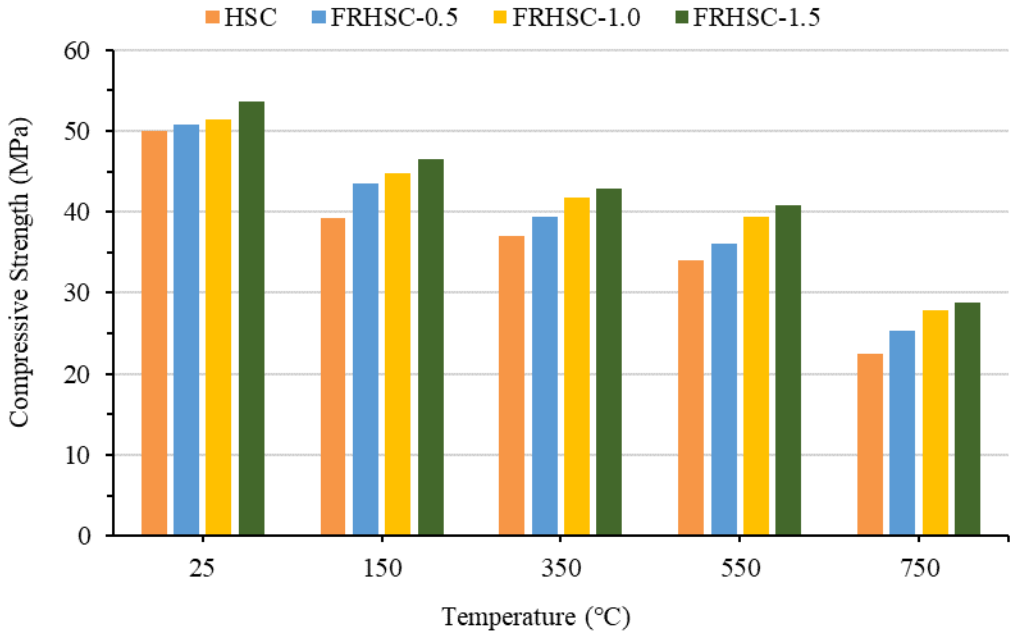

Figure 3: Compressive strength of mixes when exposed to different temperatures

3.2.2 Splitting Tensile Strength Behavior

The inspection outputs of specimens in splitting tensile strength tests for 28 days at different temperatures are highlighted in Figure 4. Likewise, compressive strength, the higher volume of PPF in test samples, ensures superior performance in the tensile strength test. Mixture FRHSC-1.5 achieved 5.08MPa, which is considerably higher than the others. Enhancement was also recorded for FRHSC-0.5 and FRHSC-1.0, amounting to 5% and 16% respectively, compared to the control HSC. Fiber actively works in mitigating crack formation and propagation, which improves tensile resistance in HSC. In one study, Afroughsabet and Ozbakkaloglu (2015) reported a 13-20% increase in tensile behavior, while in another study, the addition of 0.15-0.45% fiber with 10% silica fume resulted in a 4-9% performance improvement, as observed by Ahmed et al. (2020) after 28 days relative to the control mix. Conversely, the tensile performance of all HSC mixes started to drop noticeably with the increase in temperature. At 150°C, the decline was documented at around 14%, 13%, 10%, and 11% for HSC, FRHSC-0.5, FRHSC-1.0, and FRHSC-1.5, respectively in comparison with the ambient temperature (25°C). When the temperature went beyond 160°C, fibers within the specimens started to melt, which halted the crack dissemination. This acted as a contributing factor to the observed

variation in strength between test samples with the presence and absence of fiber reinforcement. For the subsequent two temperature stages, specimens of HSC, FRHSC-0.5, FRHSC-1.0, and FRHSC-1.5 mixtures encountered even further deterioration in strength, which accounted for 29%, 26%, 22%, and 23% at 350°C and 38%, 35%, 33%, and 34% at 550°C, respectively. Additionally, the ultimate losses were identified as approximately 50%, 47%, 44%, and 46% for HSC, FRHSC-0.5, FRHSC-1.0, and FRHSC-1.5 mixtures, respectively, when exposed to the highest temperature at 750°C. This can be explained by the physical and chemical degradation of HSC under extreme heat, as well as the coarsening effect. It was also noted that the control HSC, which contained no fiber, exhibited the most significant decrease, while FRHSC-1.0 showed the lowest percentage drop. Similar trends were observed in Behnood and Ghandehari (2009) studies, where 2 kg/m³ of PPF usage was identified as the ideal proportion in HSC at different temperatures like 100°C, 200°C, and 300°C for the relative loss in tensile strength.

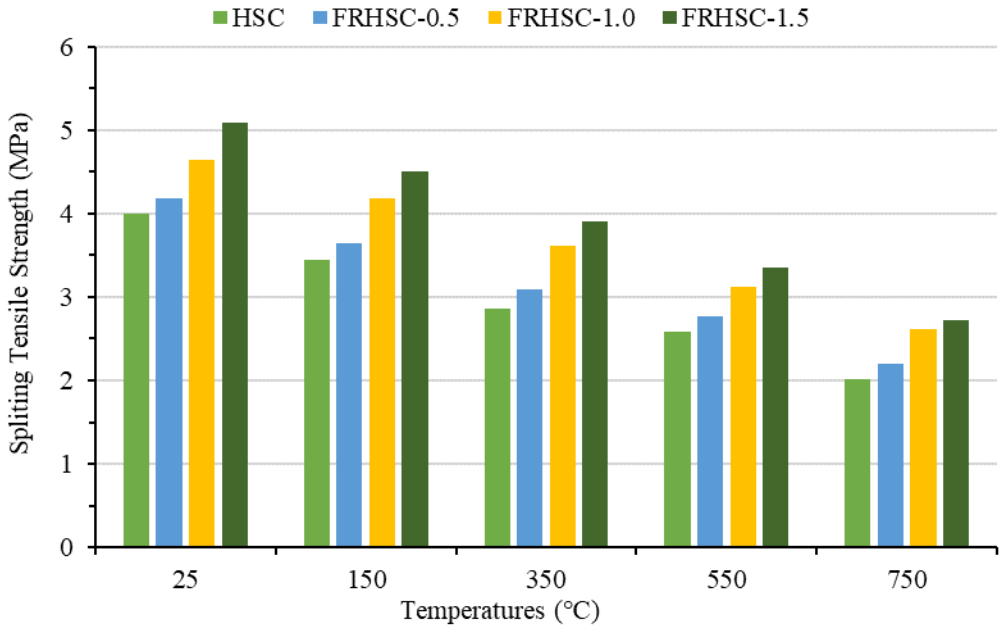

Figure 4: Tensile strength of mixes when exposed to different temperatures

3.3 Prediction Model

In the second phase of this study, a compressive strength prediction model was developed by implementing neural network concepts. In order to ensure robustness and diversity, the augmented dataset was used for training, whereas the original experimental data was utilized for cross-validation and testing of the model. To further combat overfitting, two regularization approaches were tested, including four different strength values (0, 0.01, 0.001, 0.0001) of L2 (ridge regularization) (Gupta et al., 2018), and Early Stopping (Lodwich et al., 2009). The study observed that with the sole application of early stopping with a criterion set at 10 and using an L2 regularization strength of 0, the model learned much more efficiently. Rice et al. (2020) also reported that no technique performs as well as early stopping. Lastly, the proposed ANN model generalized well with the unseen data points having an R-squared value of 0.957. Table 4 and Table 5 display the predicted values and other performance metrics individually.

Table 4: Experimental vs predicted values in MPa

Mixture type	Temperature (°C)	Experimental value (Compressive)	Predicted value (ANN)
HSC	25	50.05	46.98
	150	39.23	43.58

	350	36.96	38.16
	550	34.08	33.70
	750	22.57	22.88
FRHSC–0.5	25	50.79	47.34
	150	43.55	44.56
	350	39.4	40.11
	550	36.09	35.65
	750	25.26	24.88
FRHSC–1.0	25	51.33	49.28
	150	44.8	46.50
	350	41.82	42.05
	550	39.35	37.60
	750	27.92	26.87
FRHSC–1.5	25	53.66	53.28
	150	46.43	48.45
	350	42.86	43.99
	550	40.89	39.54
	750	28.78	29.03

Table 5: Result of different evaluation metrics

Metrics	**Result**
R^2	0.957
MSE	1.561
MAE	1.359
RMSE	1.249

4. CONCLUSIONS

Based on the insights of this study, the workability of concrete started to decline with the presence of PPF, whereas hardened properties enhanced noticeably. The impact of higher heat exposure adversely affected the strength characteristics of all mixtures, with a noticeable difference: the relative loss was less pronounced in both compressive and tensile strength for the samples containing fibers compared to the plain ones. In addition to that, specimens with 1 kg/m^3 fiber content achieved superior performance than all the other mixes. Finally, extending the dataset with 150 GN augmented data points, and the implementation of early stopping with a threshold of 10 resulted in the successful development of a robust ANN model. The compelling R-squared value of 0.957 validated the model's remarkable capability to grasp and elucidate the variations present in the data.

REFERENCES

Abuodeh, O. R., Abdalla, J. A., & Hawileh, R. A. (2020). Assessment of compressive strength of Ultra-high Performance Concrete using deep machine learning techniques. *Applied Soft Computing*, *95*, 106552. https://doi.org/https://doi.org/10.1016/j.asoc.2020.106552

Afroughsabet, V., & Ozbakkaloglu, T. (2015). Mechanical and durability properties of high-strength concrete containing steel and polypropylene fibers. *Construction and Building Materials*, *94*.

Agarap, A. F. (2018). Deep Learning using Rectified Linear Units (ReLU). *ArXiv*, *abs/1803.08375*.

Ahmadi, M., Naderpour, H., & Kheyroddin, A. (2017). ANN Model for Predicting the Compressive Strength of Circular Steel-Confined Concrete. *International Journal of Civil Engineering, 15*(2), 213-221. https://doi.org/10.1007/s40999-016-0096-0

Ahmed, T. W., Ali, A. A. M., & Zidan, R. S. (2020). Properties of high strength polypropylene fiber concrete containing recycled aggregate. *Construction and Building Materials*. https://doi.org/10.1016/j.conbuildmat.2020.118010

Almohammed, F., & Thakur, M. S. (2023). Forecasting compressive strength of concrete with basalt and polypropylene fiber by using ANN, RF and RT models. *Asian Journal of Civil Engineering*. https://doi.org/10.1007/s42107-023-00870-4

Altun, F., & Dirikgil, T. (2013). The prediction of prismatic beam behaviours with polypropylene fiber addition under high temperature effect through ANN, ANFIS and fuzzy genetic models. *Composites Part B: Engineering*, *52*, 362-371.

Bangi, M. R., & Horiguchi, T. (2011). Pore pressure development in hybrid fibre-reinforced high strength concrete at elevated temperatures. *Cement and Concrete Research*, *41*(11), 1150-1156. https://doi.org/https://doi.org/10.1016/j.cemconres.2011.07.001

Behnood, A., & Ghandehari, M. (2009). Comparison of compressive and splitting tensile strength of high-strength concrete with and without polypropylene fibers heated to high temperatures. *Fire Safety Journal*, *44*(8), 1015-1022.

Bilodeau, A., Kodur, V. K. R., & Hoff, G. C. (2004). Optimization of the type and amount of polypropylene fibres for preventing the spalling of lightweight concrete subjected to hydrocarbon fire. *Cement and Concrete Composites*, *26*(2), 163-174.

C29, A. (2017). *Standard test method for bulk density ("unit weight") and voids in aggregate*. ASTM International.

C39, A. (2020). *Standard test method for compressive strength of cylindrical concrete specimens*. ASTM International.

C127, A. (2015). *Standard test method for relative density (specific gravity) and absorption of coarse aggregate*. ASTM International.

C128, A. (2015). *Standard test method for relative density (specific gravity) and absorption of fine aggregate*. ASTM International.

C136, A. (2019). *Standard test method for sieve analysis of fine and coarse aggregates*. ASTM International.

C143, A. (2015). *Standard test method for slump of hydraulic-cement concrete*. ASTM International.

C150, A. (2020). *Standard specification for Portland cement*. ASTM International.

C192, A. (2019). *Standard practice for making and curing concrete test specimens in the laboratory*. ASTM International.

C496, A. (2017). *Standard test method for splitting tensile strength of cylindrical concrete specimens*. ASTM International.

C1116, A. (2015). *Standard specification for fiber-reinforced concrete.* ASTM International.

Caetano, H., Ferreira, G., Rodrigues, J. P. C., & Pimienta, P. (2019). Effect of the high temperatures on the microstructure and compressive strength of high strength fibre concretes. *Construction and Building Materials*, *199*, 717-736.

Choumanidis, D., Badogiannis, E., Nomikos, P., & Sofianos, A. (2016). The effect of different fibres on the flexural behaviour of concrete exposed to normal and elevated temperatures. *Construction and Building Materials*, *129*, 266-277.

El Khessaimi, Y., El Hafiane, Y., Smith, A., Tamine, K., Adly, S., & Barkatou, M. (2023). *The effectiveness of data augmentation in compressive strength prediction of calcined clay cements using linear regression learning*. https://hal.science/hal-04166948

Elsanadedy, H., Almusallam, T., Al-Salloum, Y., & Iqbal, R. (2017). Effect of high temperature on structural response of reinforced concrete circular columns strengthened with fiber reinforced polymer composites. *Journal of Composite Materials*, *51*(3), 333-355.

Gupta, S., Gupta, R., Ojha, M., & Singh, K. P. (2018, 2018//). A Comparative Analysis of Various Regularization Techniques to Solve Overfitting Problem in Artificial Neural Network. Data Science and Analytics, Singapore.

Hamrat, M., Boulekbache, B., Chemrouk, M., & Amziane, S. (2010). Shear Behaviour of RC Beams without Stirrups Made of Normal Strength and High Strength Concretes. *Advances in Structural Engineering*, *13*(1), 29-41. https://doi.org/10.1260/1369-4332.13.1.29

Huismann, S., Weise, F., Meng, B., & Schneider, U. (2012). Transient strain of high strength concrete at elevated temperatures and the impact of polypropylene fibers. *Materials and Structures*, *45*(5), 793-801. https://doi.org/10.1617/s11527-011-9798-6

Kalifa, P., Chéné, G., & Gallé, C. (2001). High-temperature behaviour of HPC with polypropylene fibres: From spalling to microstructure. *Cement and Concrete Research*, *31*(10), 1487-1499. https://doi.org/https://doi.org/10.1016/S0008-8846(01)00596-8

LeCun, Y., Bengio, Y., & Hinton, G. (2015). Deep learning. *Nature*, *521*(7553), 436-444. https://doi.org/10.1038/nature14539

LeNail, A. (2019). NN-SVG: Publication-Ready Neural Network Architecture Schematics. *J. Open Source Softw.*, *4*(33), 747.

Lodwich, A., Rangoni, Y., & Breuel, T. (2009, 14-19 June 2009). Evaluation of robustness and performance of Early Stopping Rules with Multi Layer Perceptrons. 2009 International Joint Conference on Neural Networks,

Long, P., & Nicholas, C. (2001). Mechanical Properties of High-Strength Concrete at Elevated Temperatures. In: NIST Interagency/Internal Report (NISTIR), National Institute of Standards and Technology, Gaithersburg, MD.

Meyer, D., Nagler, T., & Hogan, R. J. (2021). Copula-based synthetic data augmentation for machine-learning emulators. *Geosci. Model Dev.*, *14*(8), 5205-5215. https://doi.org/10.5194/gmd-14-5205-2021

Nath, A. D., Hoque, M. I., Datta, S. D., & Shahriar, F. (2021). Various recycled steel fiber effect on mechanical properties of recycled aggregate concrete. *International Journal of Building Pathology and Adaptation*, *ahead-of-print*(ahead-of-print). https://doi.org/10.1108/IJBPA-07-2021-0102

Noumowe, A. (2005). Mechanical properties and microstructure of high strength concrete containing polypropylene fibres exposed to temperatures up to 200 °C. *Cement and Concrete Research*, *35*(11), 2192-2198. https://doi.org/https://doi.org/10.1016/j.cemconres.2005.03.007

Noumowe, A. N., Siddique, R., & Debicki, G. (2009). Permeability of high-performance concrete subjected to elevated temperature (600°C). *Construction and Building Materials*, *23*(5), 1855-1861. https://doi.org/https://doi.org/10.1016/j.conbuildmat.2008.09.023

Ozawa, M., & Morimoto, H. (2014). Effects of various fibres on high-temperature spalling in high-performance concrete. *Construction and Building Materials*, *71*, 83-92.

Rice, L., Wong, E., & Kolter, Z. (2020). *Overfitting in adversarially robust deep learning* Proceedings of the 37th International Conference on Machine Learning, Proceedings of Machine Learning Research. https://proceedings.mlr.press/v119/rice20a.html

Roy, B., Akid, A. S. M., Sobuz, M. H. R., Shuvra, J., & Islam, M. S. (2021). Experimental investigation on mechanical performance of high-strength concrete containing polypropylene fiber exposed to high temperature. *Asian Journal of Civil Engineering*, *22*(8), 1595-1606.

Serrano, R., Cobo, A., Prieto, M. I., & González, M. d. l. N. (2016). Analysis of fire resistance of concrete with polypropylene or steel fibers. *Construction and Building Materials*, *122*, 302-309. https://doi.org/https://doi.org/10.1016/j.conbuildmat.2016.06.055

Shahriar, F., Datta, S., & Deb Nath, A. (2022). *INVESTIGATING THE MECHANICAL AND NON-DESTRUCTIVE PROPERTIES OF STEEL FIBER REINFORCED RECYCLED AGGREGATE CONCRETE*.

Singarimbun, R. N., Nababan, E. B., & Sitompul, O. S. (2019, 28-29 Nov. 2019). Adaptive Moment Estimation To Minimize Square Error In Backpropagation Algorithm. 2019 International Conference of Computer Science and Information Technology (ICoSNIKOM),

Tanyildizi, H., & Coskun, A. (2008). The effect of high temperature on compressive strength and splitting tensile strength of structural lightweight concrete containing fly ash. *Construction and Building Materials*, *22*(11), 2269-2275.

Uddin, M. N., Mahamoudou, F., Deng, B.-Y., Elobaid Musa, M. M., & Tim Sob, L. W. (2023). Prediction of rheological parameters of 3D printed polypropylene fiber-reinforced concrete (3DP-PPRC) by machine learning. *Materials Today: Proceedings*.

Varona, F. B., Baeza, F. J., Bru, D., & Ivorra, S. (2018). Influence of high temperature on the mechanical properties of hybrid fibre reinforced normal and high strength concrete. *Construction and Building Materials*, *159*, 73-82.

Ying, X. (2019). An Overview of Overfitting and its Solutions. *Journal of Physics: Conference Series*, *1168*(2), 022022. https://doi.org/10.1088/1742-6596/1168/2/022022